Astronomy & Astrophysics

A *Spitzer*-IRS view of early-type galaxies with cuspy/core nuclei and fast/slow rotation

R. Rampazzo[1], O. Vega[2], A. Bressan[3], M.S. Clemens[1], A. Marino[1], and P. Panuzzo[4]

[1] INAF Osservatorio Astronomico di Padova, Vicolo dell'Osservatorio 5, 35122 Padova, Italy
e-mail: roberto.rampazzo@oapd.inaf.it
[2] Instituto Nacional de Astrofísica, Optica y Electrónica, Apdos. Postales 51 y 216, CP 72000 Puebla, Pue., Mexico
[3] Scuola Internazionale Superiore di Studi Avanzati (SISSA), via Bonomea, 265, 34136 Trieste, Italy
[4] GEPI, Observatoire de Paris, CNRS, Univ. Paris Diderot, Place Jules Janssen, 92190 Meudon, France

ABSTRACT

Context. The recent literature suggests that an evolutionary dichotomy exists for early-type galaxies (Es and S0s, ETGs) whereby their central photometric structure (cuspy vs. core central luminosity profiles), and figure of rotation (fast vs. slow rotators), are determined by whether they were formed by "wet" or "dry" mergers.
Aims. We consider whether the mid-infrared (MIR) properties of ETGs, with their sensitivity to accretion processes in particular in the last few Gyr (on average $z \lesssim 0.2$), can put further constraints on this picture.
Methods. We investigate a sample of 49 ETGs for which nuclear MIR properties and detailed photometrical and kinematical classifications are available from the recent literature.
Results. In the stellar light cuspy/core ETGs show a dichotomy that is mainly driven by their luminosity. However, in the MIR, the brightest core ETGs show evidence that accretions have triggered both AGN and star formation activity in the recent past, challenging a dry merger scenario. In contrast, we do find in the Virgo and Fornax clusters that cuspy ETGs, fainter than $M_{K_s} = -24$, are predominantly passively evolving in the same epoch, while in low-density environments they tend to be more active.
A significant and statistically similar fraction of both fast rotators (FRs) ($38^{+18}_{-11}\%$) and slow rotators (SRs) ($50^{+34}_{-21}\%$) shows polycyclic aromatic hydrocarbon features in their MIR spectra. Ionized and molecular gas are also frequently detected. Recent star formation episodes are then a common phenomenon in both kinematical classes, even in those dominated by AGN activity, suggesting a similar evolutionary path in the last few Gyrs.
Conclusions. MIR spectra suggest that the photometric segregation between cuspy and core nuclei and the dynamical segregation between FRs and SRs must have originated before $z \sim 0.2$.

Key words. galaxies: elliptical and lenticular, cD – infrared: galaxies – galaxies: fundamental parameters – galaxies: evolution

1. Introduction

A relatively large fraction of early-type galaxies (ETGs) at high redshift show clear evidence of interaction and/or merger morphologies and active star formation (e.g. Treu et al. 2005) supporting the model view that these galaxies are produced by a halo merger process (see e.g. Mihos 2004; Cox et al. 2008; Khochfar et al. 2011; De Lucia et al. 2011, and reference therein). A further element for high redshift formation scenarios comes from their measured [α/Fe] ratios, encoding information about the timescales of star formation. In massive ETGs this ratio has super-solar values, suggesting that they formed on relatively short timescales (see e.g. Chiosi et al. 1998; Granato et al. 2004; Thomas et al. 2005; Annibali et al. 2007; Clemens et al. 2009). Annibali et al. (2007) estimated that a fair upper limit to the recent rejuvenation episodes is ~25% of the total galaxy mass, but that they are typically much less intense than that (see e.g. the *Spitzer*-IRS study of NGC 4435 by Panuzzo et al. 2007). However, rejuvenation signatures in ETGs are often detected, not only in the galaxy nucleus, but also in the disk, rings, and even in galaxy outskirts, as clearly shown by GALEX (e.g. Rampazzo et al. 2007; Marino et al. 2009, 2011; Salim & Rich 2010; Thilker et al. 2010), so that the different phases of galaxy assembly/evolution, and their link to morphological and kinematical signatures, are vivaciously debated.

The merger process may involve either relatively few major or multiple minor events during the galaxy assembly. Furthermore, it may or may not include dissipation (and star formation), two possibilities often called wet and dry mergers, respectively (see e.g. van Dokkum 2005). Other mechanisms, however, like conversion of late-type galaxies into ETGs by environmental effects, like strangulation, ram-pressure, etc. (e.g. Boselli & Gavazzi 2006), and by energy feedback from supernovae may also be important (e.g. Kormendy et al. 2009).

Two observable quantities are thought to distinguish ETGs produced by wet and dry mergers. The first, mainly the fruit of high-resolution observations with the *Hubble* Space Telescope and of high precision photometric analyses, is the presence of either a cusp or a core in the inner galaxy luminosity profile (Lauer et al. 1991, 1992; Côté et al. 2006; Turner et al. 2012). In contrast to cuspy profiles, the surface brightness in core profiles becomes shallower as $r \rightarrow 0$. The same concept is considered by Kormendy et al. (2009) who divide ETGs into cuspy-core and core-less, depending on whether the luminosity profile misses light or has an extra-light component with respect to the extrapolation of Sersic's law at small radii. Kormendy et al. (2009) suggest that cuspy-core nuclei have been scoured by binary black holes (BHs) during the last dissipationless, dry major merger. In contrast, core-less nuclei originate from wet mergers. Analogously, Côté et al. (2006) and Turner et al. (2012)

found an extra stellar nucleus in the profile decomposition of ETGs in their Virgo (ACSVCS) and Fornax (ACSFCS) surveys in addition to simple Sersic profiles, in particular in low-luminosity(/mass) ETGs. They proposed that the most important mechanism for the assembly of a stellar nucleus is the infall of star clusters through dynamical friction, while for more luminous(/massive) galaxies a wet scenario (gas accretion by mergers/accretions and tidal torques) dominates.

The second observable quantity is the kinematical class. The class is defined by a parameter describing the specific baryonic angular momentum defined as $\lambda_r = \langle r|V|\rangle / \langle r\sqrt{V^2 + \sigma^2}\rangle$, where r is the galacto-centric distance, and V and σ are luminosity weighted averages of the rotation velocity and velocity dispersion over a two-dimensional (2D) kinematical field. The measurement refers to the inner part of the galaxy, typically of the order of or less than 1 effective radius, r_e, i.e. significantly larger than the regions where cusps and cores are detected. The value λ_r divides ETGs into the two classes of fast rotators (FR) and slow rotators (SR) (Emsellem et al. 2011, and reference therein). The FRs are by far the majority of ETGs ($86 \pm 2\%$ in the ATLAS^{3D} survey) and SRs represent massive ETGs that might have suffered from significant merging without being able to rebuild a fast rotating component. Khochfar et al. (2011) find that the underlying physical reason for the different growth histories is the slowing down, and ultimately complete shut-down, of gas cooling in massive, SR galaxies. On average, the last gas-rich major merger interaction in SR happens at $z > 1.5$, followed by a series of minor mergers which build up the outer layers of the remnant, i.e. do not feed the inner part of the galaxy.

Fast rotators in the models of Khochfar et al. (2011) have different formation paths. Most of them (78%) have bulge-to-total stellar mass ratios (B/T) larger than 0.5 and manage to grow stellar discs due to continued gas cooling as a result of frequent minor mergers. The remaining 22% live in high-density environments and consist of low B/T galaxies with gas fractions below 15% that have exhausted their cold gas reservoir and have no hot halo from which gas can cool. Summarizing, a dissipative merging and/or a gas accretion episode from interacting companions, could be the way for the galaxy to rebuild a fast-rotating disk-like component. Basically, SR and FR correspond to the paradigms of dry vs. wet accretions/mergers respectively.

Recently, Lauer (2012) attempted to unite the structural and kinematical views, claiming that they are two aspects of the same process. Using the specific angular momentum $\lambda_{r_e/2}$, computed from the 2D kinematics within half the effective radius by Emsellem et al. (2011), Lauer (2012) showed that core galaxies have rotation amplitudes $\lambda_{r_e/2} \leq 0.25$ while all galaxies with $\lambda_{r_e/2} > 0.25$ and ellipticity $\epsilon_{r_e/2} > 0.2$ lack cores. Some FRs have a core profile, but they argue that both figure of rotation and the central structure of ETGs should be used together to separate systems that appear to have formed from wet and dry mergers. Krajnović et al. (2013b) show, however, that there is a genuine population of FRs with cores. They suggest that the cores of both FRs and SRs are made of old stars and are found in galaxies typically lacking molecular and atomic gas, with few exceptions.

For the sake of simplicity throughout the paper, we will call core ETGs those galaxies for which the luminosity profile shallows out as $r \rightarrow 0$ (i.e. cuspy-core in Kormendy et al. 2009; core in Lauer 2012; non-nucleated in Côté et al. 2006 and in Turner et al. 2012). We will refer to cuspy ETGs as those which present an extra central luminosity component (i.e. core-less in Kormendy et al. 2009; power-law + intermediate in Lauer 2012; nucleated in Côté et al. 2006 and in Turner et al. 2012) with

respect to a fit of a Sersic model. Depending on the accurate surface brightness profile decomposition performed by the above authors, the cuspy vs. core classification given by different authors for the same ETG is rarely discrepant.

This note aims to contribute to the debate on the origin of core/cuspy and FR/SR ETGs, and the connection to the wet vs. dry merger hypotheses, using mid-infrared (MIR) spectra of well-studied ETGs. The paper is organized as follows. In Sect. 2 we briefly describe how *Spitzer*-IRS spectra trace the recent few Gyr evolution in ETGs. We present the MIR vs. the cuspy/core nuclear properties of ETGs (Kormendy et al. 2009; Côté et al. 2006; Turner et al. 2012; Lauer 2012) in Sect. 3, and vs. the FR/SR kinematical classes (Emsellem et al. 2011) in Sect. 4. Conclusions are presented in Sect. 5.

2. A classification of *Spitzer*-IRS spectra of ETGs

Using *Spitzer*-IRS, Rampazzo et al. (2013) have recently produced an atlas of low-resolution MIR spectra of 91 nearby ($D \leq 72$ Mpc) ETGs in the Revised Shapley-Ames Catalog (RSA). Spectra are extracted within a common aperture ($3.6'' \times 18''$) providing an integral view of the galaxy's inner region. On average, the area covered by the rectangular IRS aperture is about 2–3 times the area of a circle of radius $r_e/8$. Mid-infrared spectra then cover a region where the cuspy/core profiles and/or the departures from the Sersic profile are measured, as well as a significant part of the region where FRs vs. SRs are separated, using $\lambda_{r_e/2}$, for example. In addition, dry vs. wet mergers maximize their possible signatures in the galaxy nucleus, as shown by the study of line-strength indices (e.g. Annibali et al. 2007, and references therein), by counter-rotating components (e.g. Emsellem et al. 2011) and morphological peculiarities such as irregular/chaotic dust-lanes (e.g. Côté et al. 2006; Turner et al. 2012).

For each galaxy, the atlas provides the fully reduced and calibrated spectrum, the intensity of nebular and molecular emission lines and polycyclic aromatic hydrocarbons (PAHs), after a template spectrum of a passively evolving ETG has been subtracted. Spectra are classified into five mid-infrared classes, ranging from AGN (class -4) and star forming nuclei (class 3), transition class 2 (with PAHs) and class 1 (no-PAHs) to passively evolving nuclei (class 0) (Bressan et al. 2006). Panuzzo et al. (2011) suggest that each of the five MIR classes is a snapshot of the evolution of ETG nuclei during an accretion episode, starting from, and ending with, a class 0 spectrum (see their Fig. 11). Vega et al. (2010) suggest that anomalous PAHs in class 2 spectra are produced by carbon stars which are present in stellar populations with ages in the range of a few Gyr (Nanni et al. 2013, see their Table 1), depending on the metallicity, corresponding, on average, to a redshift coverage $z \lesssim 0.2$.

Mid-infrared spectral classes show a dichotomy between the Es and S0s, i.e. the classical morphological classification provided by RSA. Rampazzo et al. (2013) found that $46^{+11}_{-10}\%$ of Es and $20^{+11}_{-7}\%$ of S0s have a spectrum of class 0, i.e. Es are significantly more passive than S0s. A small, similar ($\sim 9^{+4}_{-3}\%$) fraction of Es and S0s have PAH ratios typical of star forming galaxies. The PAHs are detected in $47^{+8}_{-7}\%$ of ETGs and with a statistically similar fraction in Es and S0s. Basically, half of ETGs ($41^{+8}_{-7}\%$) in the sample show kinematical and/or morphological scars of recent accretion episodes.

In this note we investigate ETGs subdivided into the new, well-defined photometric (cuspy vs. core) and kinematical (FR/SR) classes. To this end, we cross-correlate the MIR RSA

Table 1. The Virgo sample in Kormendy et al. (2009) with *Spitzer*-IRS MIR class.

Galaxy	RSA type	$n_{\rm tot}$	% light	$M_{K_{\rm s}}$	MIR class	Kinematical class	Kinematical and morphological peculiarities	Dust
Core			Missing light					
NGC 4472	E1/S0$_1$(1)	$5.99^{+0.31}_{-0.29}$	-0.50 ± 0.05	-25.73	1	SR	CR s-s (1)	Y
NGC 4486	E0	$11.84^{+1.79}_{-1.19}$	-4.20 ± 1.00	-25.31	4	SR	SC(2), jet	Y
NGC 4649	S0$_1$(2)	$5.36^{+0.38}_{-0.32}$	-1.05 ± 0.07	-25.35	1	FR	asym. rot. curve (6)	N
NGC 4365	E3	$7.11^{+0.40}_{-0.35}$	-0.63 ± 0.07	-25.19	0	SR	Faint SW fan (4)	N
NGC 4374	E1	$7.98^{+0.71}_{-0.56}$	-1.52 ± 0.05	-25.13	2	SR	$V \approx 0$ (3); SC (2)	Y
NGC 4261	E3	$7.49^{+0.82}_{-0.60}$	-1.84 ± 0.05	-25.24	4	SR	NW tidal arm, faint SE fan (4)	Y
NGC 4382	S0$_1$(3) pec	$6.12^{+0.31}_{-0.27}$	-0.18 ± 0.06	-25.13	1	FR	MC(2), shells (7)	Y
NGC 4636	E0/S0$_1$(6)	$5.65^{+0.48}_{-0.28}$	-0.22 ± 0.04	-24.42	2	SR	gas irr. motion (a)	Y
NGC 4552	S0$_1$(0)	$9.22^{+1.13}_{-0.83}$	-1.23 ± 0.09	-24.31	2	SR	KDC (2) shells (4)	Y
Cuspy			Extra light					
NGC 4621	E5	$5.36^{+0.30}_{-0.28}$	0.27 ± 0.06	-24.13	0	FR	KDC (2)	N
NGC 4473	E5	$4.00^{+0.18}_{-0.16}$	8.80 ± 1.00	-23.77	0	FR	MC (2)	N
NGC 4478	E2	$2.07^{+0.08}_{-0.07}$	1.12 ± 0.15	-23.15	0	FR	. . .	N
NGC 4570	S0$_1$(7)/E7	3.69 ± 0.50	. . .	-23.49	0	FR	MC (2)	N
NGC 4660	E5	4.43 ± 0.38	. . .	-22.69	0	FR	MC (2)	N
NGC 4564	E6	4.69 ± 0.20	. . .	-23.09	0	FR	SC (2)	N

Notes. Core and cuspy galaxies correspond to cuspy-core and core-less, respectively, in Kormendy et al. (2009). The Sersic's index, $n_{\rm tot}$, and the percentage of extra light are taken from Kormendy et al. (2009). The $M_{K_{\rm s}}$ absolute magnitude and the MIR class is obtained from Brown et al. (2011) and Rampazzo et al. (2013). Kinematical classes are from Emsellem et al. (2011). Kinematical and morphological peculiarities are coded as follows: CR s-s: counter rotation stars vs. stars (1) Corsini et al. (1998); KDC indicates a kinematically decoupled component, not necessarily counter-rotation; MC multiple components; SC single component Krajnović et al. (2008); (2) A description of the kinematic and morphological peculiarities of the galaxies and full references are reported in: (3) Emsellem et al. (2004); (4) Tal et al. (2009); (5) Malin & Carter (1983); (6) Pinkney et al. (2003); (7) Kormendy et al. (2009). Dust properties (Y if present) are taken from Côté et al. (2006) and Table B3 in Rampazzo et al. (2013).

sample described above with the Kormendy et al. (2009), Lauer (2012), Côté et al. (2006), Turner et al. (2012), and ATLAS$^{\rm 3D}$ samples (see e.g. Emsellem et al. 2011, and references therein) to investigate the recent nuclear star formation history. Fourteen ETGs in Virgo, in particular the brighter ones, are in common with Kormendy et al. (2009) who classified them as either cuspy-core or core-less (i.e. core and cuspy in the present paper); 26 are in common with the ACSVCS+ACSFCS surveys in which galaxies are separated into core+Sersic and Sersic type nuclei (Côté et al. 2006; Turner et al. 2012); and 41 out of 91 ETGs in the RSA MIR atlas are in common with the ATLAS$^{\rm 3D}$ survey sample. For these galaxies Emsellem et al. (2011) provide a classification of FR or SR. The inner luminosity profiles of these ETGs have been classified into cuspy (power-law and intermediate) or core by Lauer (2012) (23 out of 41) and by Krajnović et al. (2013b) for a total of 44 objects.

3. MIR spectra vs. nuclear features in ETGs

3.1. The Virgo sample of Kormendy et al. (2009)

The structural and photometric properties of a sample of Es (some galaxies are classified S0 in the Revised Shapley Ames Catalogue Sandage & Tammann 1987 as shown in Table 1) in the Virgo cluster have been well studied by Kormendy et al. (2009). The authors divided their sample according to departures at small radii from the Sersic, $\log I \propto r^{1/n}$, law. Ten Es with total absolute magnitudes $M_{VT} \leq -21.66$, i.e. the brightest objects of their sample, have core luminosity profiles. This class of ETGs miss light with respect to the extrapolation of Sersic's law at small radii. Seventeen fainter galaxies, mostly Es in RSA, in the

magnitude range $-21.54 \leq M_{VT} \leq -15.53$, are cuspy, having excess light in their centre with respect to the inward extrapolation of the outer Sersic profile.

With the exception of NGC 4406, all core ETGs in the Kormendy et al. (2009) sample, listed in the top part of Table 1, have a MIR spectrum in the RSA sample of Rampazzo et al. (2013). The IRS spectra are also available for three cuspy ETGs, namely NGC 4621, NGC 4473 and NGC 4478; NGC 4570, NGC 4660, and NGC 4564, having absolute magnitudes similar to that of NGC 4478, also have IRS spectra, but values for the extra light component have not been quantified by Kormendy et al. (2009). We have collected the basic data in Table 1.

According to Kormendy et al. (2009), core and cuspy ETGs have fundamentally different properties. Core ETGs are slowly rotating, have anisotropic velocity distributions, boxy isophotes, Sersic index $n > 4$, and are α-element enhanced, i.e. their stellar populations formed on short timescales. In contrast, cuspy ETGs rotate rapidly, are more isotropic and have disky isophotes. They tend to have lower values of the Sersic index, $n \simeq 3 \pm 1$, and be less α-enhanced. All cuspy ETGs are fast rotators, while most (7 out of 9) of core Es are slow rotators within $r_{\rm e}/2$ (Emsellem et al. 2011) (Table 1, Col. 7).

The MIR spectra of the subset of Kormendy et al. (2009) ETGs is shown in Fig. 1. All cuspy galaxies have a passive, class 0 spectrum characterized by the 10 μm silicon feature produced by oxygen rich AGB stars. Their kinematics show signatures of past interaction/accretion episodes, such as kinematically decoupled cores (KDC) and multiple velocity components (MC). All have low nuclear X-ray luminosities ($38.18 \leq \log L_{\rm X,nucl} \leq 38.92$ erg s^{-1}, Pellegrini 2010) indicating that no
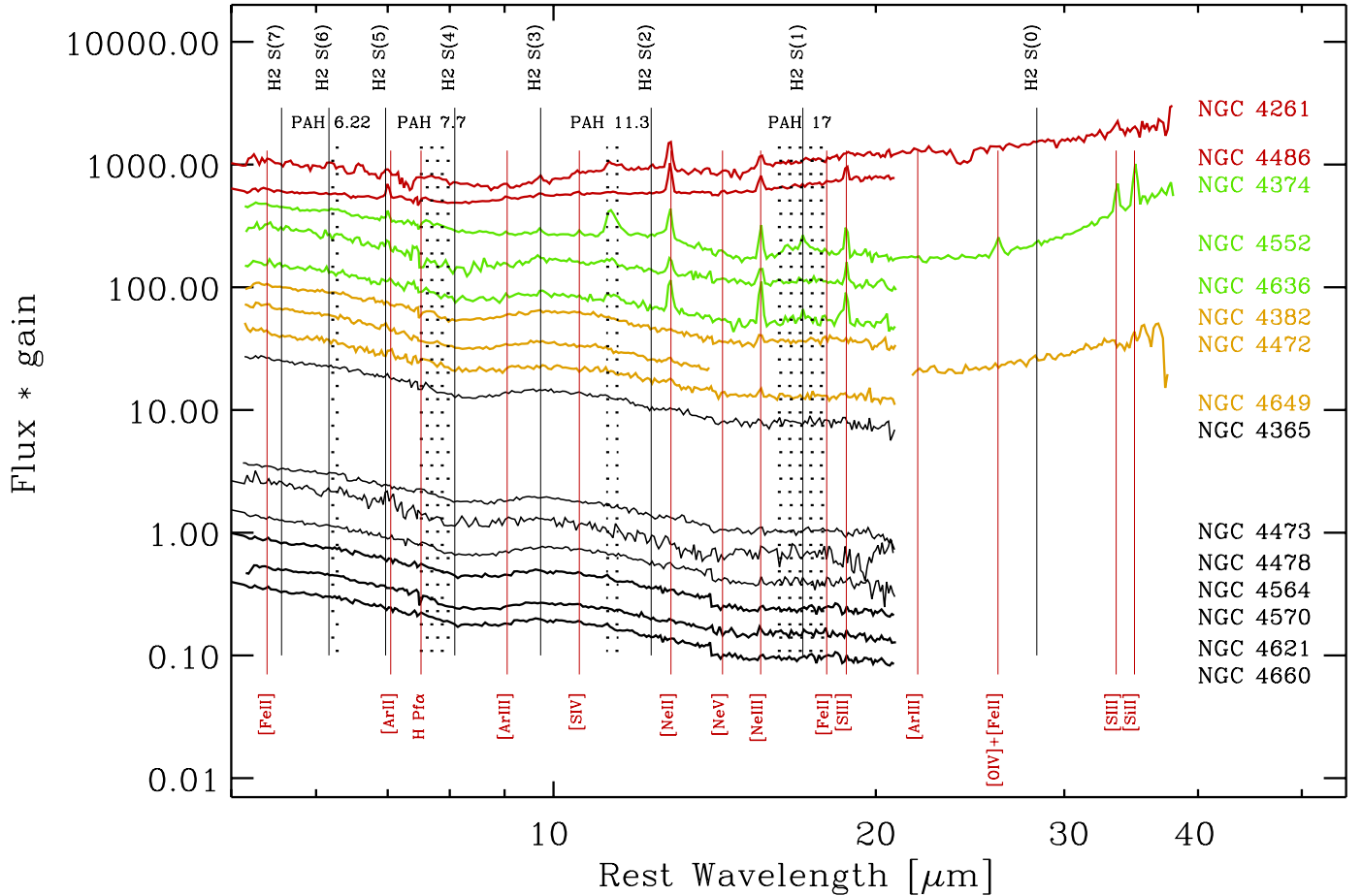
Fig. 1. ETGs in the sample of Kormendy et al. (2009). MIR classes are colour coded (black = class 0; yellow = class 1; green = class 2; and red = class 4. Nebular lines in the spectra are indicated with vertical red solid lines. PAH complexes are indicated with dotted areas. H_2 rotational emission lines are indicated with black solid lines.

AGN are active, as also supported by the low radio power at 1.4 GHz (most are upper limits while NGC 4563 has $P_{1.4\ GHz} = 4.9 \times 10^{19}$ W Hz^{-1}, Brown et al. 2011) (see also Rampazzo et al. 2013, Table B.1).

A more active picture emerges for core ETGs. The MIR spectra indicate nuclei with different kinds of activity from AGN (class 4, M 87, and NGC 4261) to post-star forming (MIR class 2 with anomalous PAHs, NGC 4374, NGC 4636, NGC 4552) to the quiescent nucleus of NGC 4365 (class 0).

Most SRs and FRs show signatures of kinematical and morphological peculiarities suggesting the action of accretion episodes. Of particular interest is NGC 4382; although it shows strong shell features (see e.g. Fig. 9 in Kormendy et al. 2009) it has a nearly passively evolving nucleus (class 1). This is not the case for NGC 4374 and NGC 4552, which both show fine structure (see Sansom, Hibbard & Schweizer 2000), although less prominent than that in NGC 4382. The class 2 spectrum of NGC 4552 reveals the presence of gas and the additional presence of anomalous PAHs, as in NGC 4374, points to the occurrence of a recent star formation event.

Summarizing, there is evidence that accretions in the brightest, core Es in the Kormendy et al. (2009) sample have triggered both AGN and SF activity, a challenge for completely dry mergers/accretions in the last few Gyrs. In contrast, the few cuspy galaxies in the present MIR sample are all passively evolving. They may have either been quiescent for a very long time (the radio power may take longer to vary; see e.g. Brown et al. 2011) or possible accretions have been "sterile", i.e. activating neither

AGN nor star formation. An additional hint of a different recent evolution of the two photometric classes may come from the observation that dust appears to be totally absent in cuspy ETGs, while most of the core ETGs do show dust (Col. 9 in Table 1). Clemens et al. (2010) found that dust can survive no longer than a few tens of Myr in the hostile ETG environment, so if present, should be quite recently acquired.

3.2. The ACS Virgo and Fornax ETGs samples

The passive evolution of all six of the fainter *cuspy* ETGs in our subset of the Kormendy et al. (2009) sample prompted us to enlarge the sample to fainter galaxies. A large HST study of the inner regions of ETGs in the Virgo and Fornax clusters has been performed by Côté et al. (2006) and Turner et al. (2012), the ACSVCS and ACSFCS, respectively. The final sample with MIR spectra includes 23 ETGs in Virgo (top part of Table 2) and 8 ETGs in Fornax (bottom of Table 2) that have been classified by Turner et al. (2012) with an ACS class of either core (originally non-nucleated) or cuspy (originally nucleated). Additional ETGs in low-density environments, with a MIR spectrum in Rampazzo et al. (2013) and a Sersic decomposition of the luminosity profile, come from Krajnović et al. (2013b) and are listed in Table 2.

In Fig. 2 we plot the absolute K_s-band magnitude distribution of cuspy and core ETGs in the Virgo and Fornax clusters (bottom-left panel) and of the entire sample (bottom-right

Table 2. The sample of ATLAS^{3D} ETGs with a *Spitzer*-IRS class.

Galaxy	Morpho. RSA	T	P	$\lambda_{r_e/2}$	$\epsilon_{r_e/2}$	$V/\sigma_{r_e/2}$	FR/SR$_{r_e/2}$ class	n_{tot}	MIR class
NGC 821	E6	-4.8 ± 0.4	cuspy	0.27	0.39	0.29	FR	10.4 ± 0.7	0
NGC 2685	S0$_3$(7) pec	-1.0 ± 0.8	cuspy	0.63	0.19	0.73	FR	4.3 ± 0.4	2
NGC 2974	E4	-4.2 ± 1.2	cuspy	0.66	0.40	0.81	FR	4.0 ± 0.4	2
NGC 3193	E2	-4.8 ± 0.5	core	0.20	0.14	0.21	FR	5.3 ± 0.1	0
NGC 3245	S0$_1$	-2.1 ± 0.5	cuspy	0.59	0.44	0.58	FR	3.2 ± 1.9	3
NGC 3377	E6	-4.8 ± 0.4	cuspy	0.52	0.50	0.56	FR	5.0 ± 0.5	0
NGC 3379	E0	-4.8 ± 0.5	core	0.16	0.10	0.15	FR	5.3 ± 0.9	0
NGC 3608	E1	-4.8 ± 0.5	core	0.04	0.19	0.05	SR	3.9 ± 0.5	0
NGC 4036	S0$_3$(8)/Sa	-2.6 ± 0.7	. . .	0.68	0.54	0.80	FR	2.0 ± 0.1	2
NGC 4261	E3	-4.8 ± 0.4	core	0.09	0.22	0.09	SR	5.1 ± 0.4	4
NGC 4339	S0$_{1/2}$(0)	-4.7 ± 0.8	cuspy	0.31	0.06	0.30	FR	4.1 ± 0.6	0
NGC 4365	E3	-4.8 ± 0.5	core	0.09	0.25	0.11	SR	5.2 ± 0.4	0
NGC 4371	SB0$_{2/3}$(r)(3)	-1.3 ± 0.6	cuspy	0.48	0.31	0.54	FR	3.8 ± 0.6	2
NGC 4374	E1	-4.3 ± 1.2	core	0.02	0.15	0.03	SR	6.0 ± 0.3	2
NGC 4377	S0$_1$(3)	-2.6 ± 0.6	cuspy	0.34	0.23	0.31	FR	2.2 ± 1.2	0
NGC 4382	S0$_1$(3) pec	-1.3 ± 0.6	core	0.16	0.20	0.17	FR	5.1 ± 1.3	1
NGC 4435	SB0$_1$(7)	-2.1 ± 0.5	. . .	0.60	0.46	0.67	FR	4.7 ± 0.3	3
NGC 4442	SB0$_1$(6)	-1.9 ± 0.4	cuspy	0.34	0.31	0.33	FR	2.8 ± 0.2	0
NGC 4472	E1/S0$_1$(1)	-4.8 ± 0.5	core	0.08	0.17	0.07	SR	4.7 ± 0.1	1
NGC 4473	E5	-4.7 ± 0.7	core	0.25	0.40	0.26	FR	5.7 ± 0.5	0
NGC 4474	S0$_1$(8)	-2.0 ± 0.5	cuspy	0.35	0.47	0.35	FR	3.5 ± 0.4	2
NGC 4477	SB0$_{1/2}$/SBa	-1.9 ± 0.4	cuspy	0.22	0.13	0.21	FR	4.1 ± 1.2	2
NGC 4478	E2	-4.8 ± 0.4	core	0.18	0.17	0.17	FR	2.0 ± 0.1	0
NGC 4486	E0	-4.3 ± 0.6	core	0.02	0.04	0.02	SR	2.9 ± 0.2	4
NGC 4550	E7/S0$_1$(7)	-2.1 ± 0.7	cuspy	0.06	0.63	0.07	SR	1.7 ± 0.1	3
NGC 4552	S0$_1$(0)	-4.6 ± 0.9	core	0.05	0.05	0.05	SR	6.2 ± 0.4	2
NGC 4564	E6	-4.8 ± 0.5	cuspy	0.54	0.48	0.53	FR	2.9 ± 0.2	0
NGC 4570	S0$_1$(7)/E7	-2.0 ± 0.7	cuspy	0.50	0.55	0.47	FR	2.4 ± 0.2	0
NGC 4621	E5	-4.8 ± 0.5	cuspy	0.29	0.36	0.27	FR	4.3 ± 0.2	0
NGC 4636	E0/S0$_1$(6)	-4.8 ± 0.5	core	0.04	0.09	0.04	SR	5.5 ± 0.5	2
NGC 4649	S0$_1$(2)	-4.6 ± 0.8	core	0.13	0.16	0.12	FR	5.1 ± 0.5	1
NGC 4660	E5	-4.7 ± 0.5	cuspy	0.47	0.32	0.52	FR	3.5 ± 0.2	0
NGC 4697	E6	-4.4 ± 0.8	cuspy	0.47	0.32	0.36	FR	4.6 ± 0.2	3
NGC 5273	S0/a	-1.9 ± 0.4	cuspy	0.48	0.12	0.51	FR	1.8 ± 1.1	4
NGC 5353	S0$_1$(7)/E7	-2.1 ± 0.6	. . .	0.53	0.54	0.54	FR	3.3 ± 0.5	2
NGC 5631	S0$_3$(2)/Sa	-1.9 ± 0.4	. . .	0.17	0.17	0.19	FR	4.3 ± 0.5	2
NGC 5638	E1	-4.8 ± 0.4	. . .	0.23	0.08	0.22	FR	3.5 ± 0.2	0
NGC 5813	E1	-4.8 ± 0.4	core	0.07	0.17	0.16	SR	5.8 ± 1.7	1
NGC 5831	E4	-4.8 ± 0.5	cuspy	0.06	0.20	0.16	SR	4.3 ± 0.2	0
NGC 5846	S0$_1$(0)	-4.7 ± 0.7	core	0.03	0.06	0.04	SR	3.9 ± 0.2	1
NGC 7332	S0$_{2/3}$	-1.9 ± 0.5	cuspy	0.34	0.44	0.29	FR	2.3 ± 0.4	1
NGC 1339	E4	-4.3 ± 0.5	cuspy	. . .	. . .	. . .	. . .	. . .	0
NGC 1351	S0$_1$(6)/E6	-3.1 ± 0.6	core	. . .	. . .	. . .	. . .	. . .	0
NGC 1374	E0	-4.4 ± 1.1	core	. . .	. . .	. . .	. . .	. . .	0
NGC 1389	S0$_1$(5)/SB0$_1$	-2.8 ± 0.7	cuspy	. . .	. . .	. . .	. . .	. . .	0
NGC 1399	E1	-4.6 ± 0.5	core	. . .	. . .	. . .	. . .	. . .	0
NGC 1404	E2	-4.8 ± 0.5	core	. . .	. . .	. . .	. . .	. . .	1
NGC 1427	E5	-4.0 ± 0.9	core	. . .	. . .	. . .	. . .	. . .	0
IC 2006	E1	-4.2 ± 0.9	cuspy	. . .	. . .	. . .	. . .	. . .	1

Notes. ETGs in ATLAS^{3D} (top part of the table), including the Virgo sample, plus Fornax cluster ETGs (Turner et al. 2012) represent the global sample used for the core vs. cuspy and FR vs. SR analyses. Morphological classifications in Cols. 2 and 3 are from RSA and LEDA, respectively. For the ATLAS^{3D} sample, the profile type (Col. 4), P, is cuspy (originally \ = power law, ∧ = intermediate) and core (originally ∩) is taken from Krajnović et al. (2013b). The specific angular momentum (Col. 5), $\lambda_{r_e/2}$; the ellipticity (Col. 6), $\epsilon_{r_e/2}$; the rotation velocity to velocity dispersion ratio (Col. 7), $V/\sigma_{r_e/2}$; and the kinematical class (Col. 8), FR/SR, at $r_e/2$ are from Emsellem et al. (2011). The Sersic index (Col. 9), n_{tot}, is from Krajnović et al. (2013a). The MIR class (Col. 10) is taken from Rampazzo et al. (2013).

panel). Côté et al. (2006) and Turner et al. (2012) noticed that virtually none of the bright ETGs are cuspy, in contrast to the fainter ones, as shown by the lower panel in Fig. 2. The percentage of cuspy ETGs in Virgo and Fornax reaches $67\% \pm 8\%$ and $72\% \pm 13\%$, respectively, among fainter galaxies in their sample. In the top-left panel of Fig. 2 we show the distribution of MIR classes in the same bins of M_K magnitude. Most of the cuspy

ETGs have MIR class 0 spectra, indicating passive evolution in their nucleus. Considering ETGs with $M_K \geq -24$, $82^{+18}_{-16}\%$[1] of the galaxies are cuspy, of which $59^{+25}_{-18}\%$ are passively evolving and only $18^{+17}_{-10}\%$ show PAH features. The brightest ($M_K \leq -25$)

[1] The fractions reported consider upper and lower errors corresponding to 1σ Gaussian errors (Gehrels 1986).
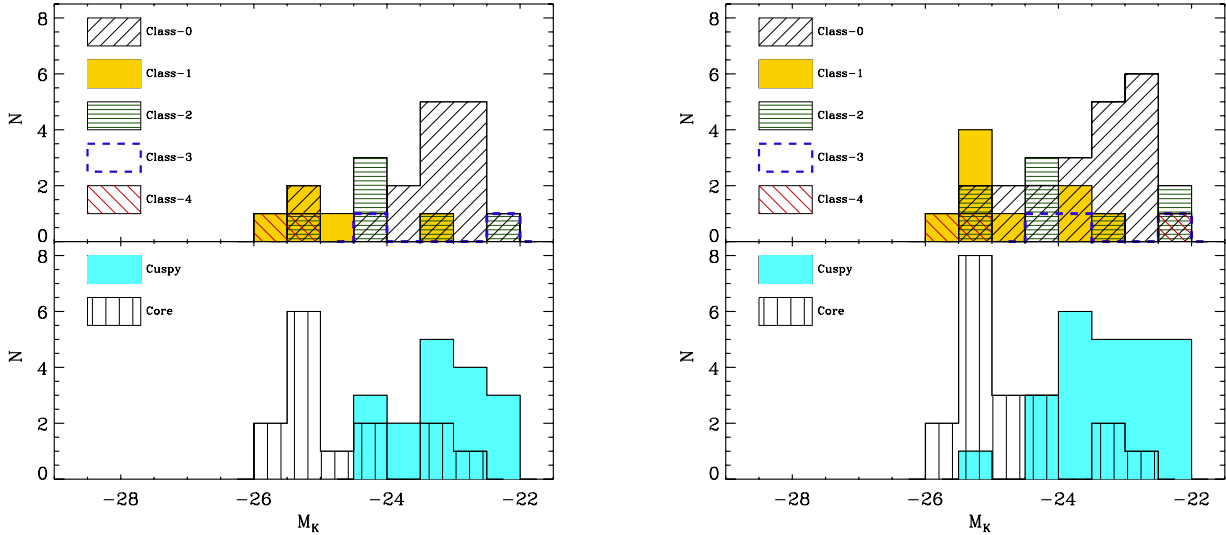
Fig. 2. K_s-band absolute magnitude, M_K, distribution vs. MIR classes (*top panels*) and cuspy/core ETGs in the Virgo plus Fornax clusters (Côté et al. 2006; Turner et al. 2012) (*left panel*) and in the total sample, including ETGs in low-density environments in Krajnović et al. (2013b).

ETGs have cores, and various MIR spectra are found, from class 0 to class 4, as noticed before in the Kormendy et al. (2009) sample. However, active MIR classes, 1–4, are distributed along all the M_K range examined, suggesting that wet accretions occur at the entire magnitude/mass bins.

In the right panels of Fig. 2 we consider the entire sample of 44 ETGs with a MIR spectrum and a core/cuspy classification. Of the whole sample, 62^{+22}_{-15}% of the passive ETGs are cuspy. For the subset fainter than $M_K = -24$, 87^{+23}_{-18}% are *cuspy*, 57^{+22}_{-16}% are passively evolving, and 33^{+18}_{-12}% show PAHs in their MIR spectra. Although the increase in the number of galaxies is modest going from cluster to low-density environments, the number of active galaxies (classes 1, 2, 3 and 4) tends to increase at all magnitude/mass bins, suggesting a possible environmental effect (see e.g. Clemens et al. 2006, 2009). Serra et al. (2012) detected HI in 40% of ETGs outside Virgo and 10% inside it.

4. MIR spectra vs. fast and slow rotators

With the aim of investigating the MIR properties of FRs vs. SRs in the $r_e/2$ region, we cross-correlate the samples adding a measure of the specific angular momentum to our sample with a MIR nuclear classification. In the Rampazzo et al. (2013, Table 5) sample of MIR spectra, 41 out of 91 ETGs have a measure of the specific angular momentum. Table 2 provides the list of ETGs with a FR/SR classification within $r_e/2$ (Col. 8 from Emsellem et al. 2011, ATLAS^{3D}: Table B1) and their MIR class (Col. 10). The list includes 29 FRs and 12 SRs. The Fornax ETGs lack the kinematical classification in the $r_e/2$ region.

In Fig. 3 the specific angular momentum at $r_e/2$, $\lambda_{r_e/2}$, is plotted against the corresponding average ellipticity, $\epsilon_{r_e/2}$, (Table 2, Cols. 5 and 6). According to Lauer (2012) the dashed line in the figure separates the core and cuspy ETGs into different rotation classes, leaving the core set contaminated only by face-on cuspy galaxies. The figure shows the 23 galaxies of Lauer (2012), among the 41 ETGs in Emsellem et al. (2011) (large squares for SRs, large circles for FRs). Figure 3 plainly shows that different MIR classes are found associated with both FRs and SRs, as well as in core and cuspy ETGs.

The fraction of SRs and FRs with a class 0 spectrum, i.e. that are passively evolving, is 25^{+24}_{-14}% and 52^{+17}_{-13}%, respectively.

This means that the fraction of SRs and FRs showing emission lines (MIR classes 1, 2, 3, and 4), i.e. the complement of passive ETGs, 75^{+25}_{-24}% and 48^{+17}_{-12}%, respectively. In the whole Rampazzo et al. (2013) sample, 64^{+12}_{-6}% of the nuclei show emission lines, although with different intensity. These results are in agreement with optical studies in which, depending on the sample, the ionized gas is detected in ≈50–90% of ETGs (Phillips et al. 1986; Macchetto et al. 1996; Sarzi et al. 2006, 2010; Yan et al. 2006; Serra et al. 2008; Annibali et al. 2010). This suggests that *wet-mergers/accretions* have played a role in the last few Gyrs of both SRs and FRs.

The fraction of SRs and FRs showing PAH features (MIR classes 2, 3, and 4) is 50^{+30}_{-20}% and 38^{+15}_{-11}%, respectively, indicating that in about half of both SRs and FRs a star formation episode has recently occurred (Kaneda et al. 2008; Panuzzo et al. 2011; Rampazzo et al. 2013). Galaxies with normal PAH ratios, class 3 spectra, are in the minority: only 10^{+8}_{-5}% of FRs show star forming spectra and 8^{+19}_{-2}% SRs. All MIR class 4 spectra, 17^{+22}_{-11}% of SRs and 3^{+8}_{-1}% of FRs, show PAHs. The optical study of 65 ETGs of Annibali et al. (2010) provided indications that the AGN phenomenon is associated with star formation.

5. Summary and conclusions

This note investigates whether the photometric segregation between cuspy and core nuclei and/or the dynamical segregation between fast and slow rotators can be attributed to formation via wet or dry mergers.

We explore the question by comparing the MIR spectral characteristics with their cuspy/core morphology (Kormendy et al. 2009; Lauer 2012; Côté et al. 2006; Turner et al. 2012; Krajnović et al. 2013a) and FR/SR characterization (ATLAS^{3D}). We use the *Spitzer*-IRS spectra and MIR classes discussed in Panuzzo et al. (2011) and Rampazzo et al. (2013). These spectra are sensitive to the last few Gyrs ($z \lesssim 0.2$) of the ETGs evolution. We find the following:

– With the exception of NGC 4365, which is passively evolving, MIR spectra of all the bright core ETGs in the Kormendy et al. (2009) sample show nebular emission lines, and PAH features are detected in 5 out of 9 objects. These
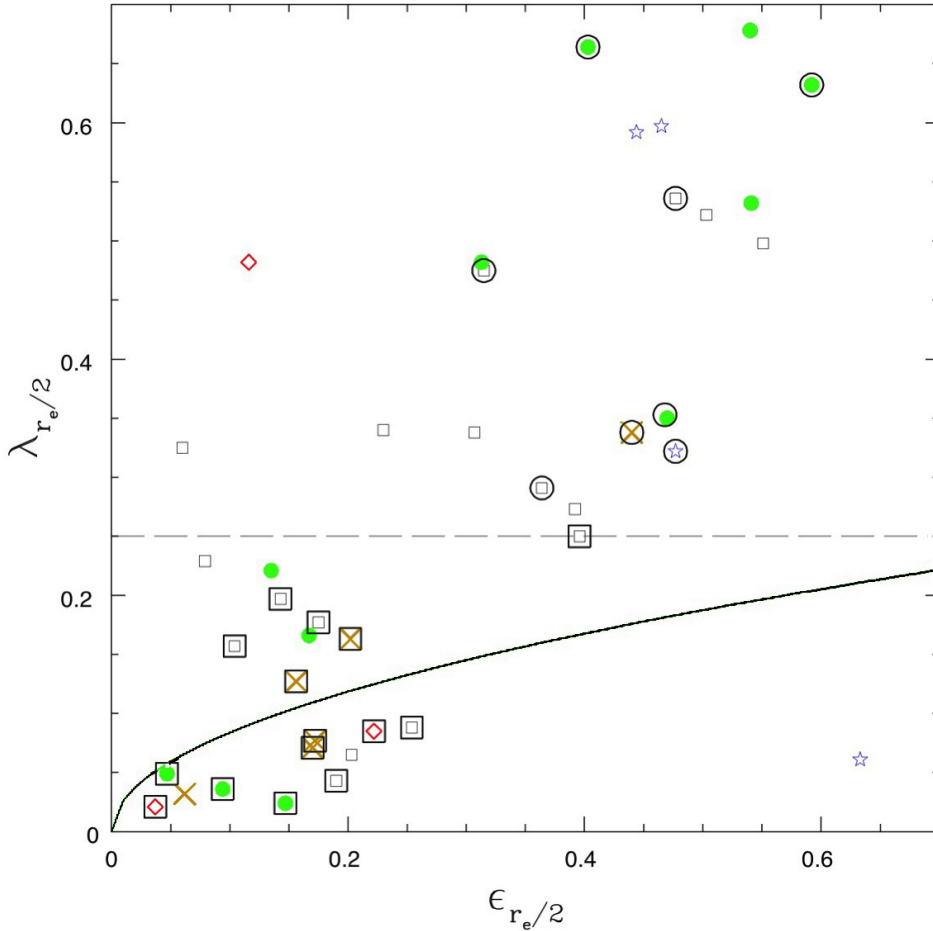
Fig. 3. Specific baryonic angular momentum, $\lambda_{r_e/2}$, vs. average ellipticity, $\epsilon_{r_e/2}$, measured for the 41 ETGs in Table 2 (see references in the table caption.) The solid line separates FRs from SRs according to Emsellem et al. (2011). The dashed line separates ETGs with cuspy profiles (large circles) from core galaxies (large squares) in the sample of Lauer (2012). MIR classes are coded as follows: square = class 0; cross = class 1; full dot = class 2; star = class 3, and diamonds = class 4.

types of nuclei should have recently accreted gas-rich material. If these objects formed via dry mergers, the process was completed before $z \sim 0.2$ and wet accretions have happened since; AGN feedback does not prevent a late star formation episode in the bright Es NGC 4374, NGC 4636, and NGC 4552. The few (6) faint, cuspy ETGs in the Kormendy et al. (2009) sample all show passively evolving spectra, irrespective of their magnitude.

- The MIR spectra of the total cuspy/core sample (44 ETGs), confirm that ETGs fainter than $M_{K_s} = -24$ mag, mostly cuspy, are predominantly passively evolving. This fact is particularly significant in Virgo and Fornax where $82^{+18}_{-10}\%$ are cuspy, the majority also FRs. Kormendy et al. (2009) noticed that cuspy ETGs have disky (positive a_4/a Fourier coefficient) isophotes in the nuclear region, a structure that suggests some form of dissipation during the formation. The passive MIR spectra suggest that either this infall was sterile, i.e. without star formation, or happened at $z \gtrsim 0.2$, so as to leave no trace in the present MIR spectra. The Khochfar et al. (2011) models suggest that a fraction of FRs lying in high-density environments have a residual gas fraction below 15%, i.e. they have exhausted their cold gas reservoir and have no hot halo from which gas can cool. Counterparts in low-density environments (Fig. 2, right panel) show the tendency to be more gas rich and hence more active.

- A significant fraction of both FRs ($38^{+18}_{-11}\%$) and SRs ($50^{+34}_{-21}\%$) shows PAH features in their MIR spectra. Ionized and molecular gas are also commonly detected. Recent star formation episodes are not a rare phenomenon in either FRs or SRs, even in those dominated by AGN activity (see also,

Annibali et al. 2010). Recently, observing HI rich ETGs, Serra et al. (2014) found that SRs are detected as often, host as much H I and have a similar rate of H I discs/rings as FRs.

Despite the expectation that the signature of wet or dry merger is strongest in the galaxy nucleus, the nuclear MIR spectra do not clearly link the core versus cuspy morphology and the FR versus SR kinematical class to these alternative formation scenarios. Within the last few Gyrs, only at the two extremes of the ETG luminosity, does the dichotomy emerge: the brightest core, mostly SRs and faint cuspy, mostly FRs (in the Virgo and Fornax clusters) separate into mostly active and passive ETGs, respectively. The result, however, is in contrast to what is expected for core-SR versus cuspy-FR, i.e. a dry vs. wet accretion scenario.

The obvious possibility is that these photometric and kinematical classes are signatures generated by the two different evolutionary scenarios at $z \gtrsim 0.2$ (see e.g. Khochfar et al. 2011), so that they do not affect the MIR spectra. On the other hand, adopting the traditional E/S0s morphological subdivision Rampazzo et al. (2013) found that Es are significantly more passive than S0s in the same epoch. Fast/Slow rotator classes may smooth away differences between Es and S0s, since a large fraction of Es transit into the FR class. At the same time, recent observations tend to emphasize the complexity of ETGs when their study is extended to large radii (see also Serra et al. 2014). Arnold et al. (2014) recently obtained the extended, up to 2–4 r_e, kinematics of 22 ETGs in RSA. They find that only SRs remain slowly rotating in their halos, while the specific angular momentum of ETGs classified as FRs within $r_e = 1$, may dramatically change at larger radii. Arnold et al. (2014) suggest that the traditional E/S0

classification better accounts for the observed kinematics up to large radii and likely of their complex evolutionary scenario.

References

Annibali, F., Bressan, A., Rampazzo, R., Zeilinger, & Danese, L. 2007, A&A, 463, 455

Annibali, F., Bressan, A., Rampazzo, R., et al. 2010, A&A, 519, A40

Arnold, J. A., Romanowsky, A. J., Brodie, J. P., et al. 2014, ApJ, submitted [arXiv:1310.2607]

Boselli, A., & Gavazzi, G. 2006, PASP, 118, 517

Bressan, A., Panuzzo, P., Buson, L., et al. 2006, ApJ, 639, L55

Brown, M. J. I., Januzzi, B. T., Floyd, D. J. E., & Mould, J. R. 2011, ApJ, 731, L41

Chiosi, C., Bressan, A., Portinari, L., & Tantalo, R. 1998, A&A, 339, 355

Clemens, M. S., Bressan, A., Nikolic, B., et al. 2006, MNRAS, 370, 702

Clemens, M. S., Bressan, A., Nikolic, B., & Rampazzo, R. 2009, MNRAS, 392, L35

Clemens, M. S., Jones, A. P., Bressan, A., Baes, Bendo, M. G. J., et al. 2010, A&A, 518, L50

Corsini, E. M., & Bertola, F. 1998, J. Korean Phys. Soc., 33, 574

Côté, P., Slawomir, P., Ferrarerse, L., et al. 2006, ApJS, 165, 57

Cox, T. J., Jonsson, P., Somerville, R. S., Primack, J. R., & Dekel, A. 2008, MNRAS, 384, 386

De Lucia, G., Fontanot, F., Wilman, D., & Monaco, P. 2011, MNRAS, 414, 1439

Emsellem, E., Cappellari, M. Peletier, R. F., McDermid, R. M., & Bacon, R. 2004, MNRAS, 352, 721

Emsellem, E., Cappellari, M., Krajnović, D., et al. 2011, MNRAS, 414, 888

Gehrels, N. 1986, ApJ, 303, 336

Granato, G. L., De Zotti, G., Silva, L., Bressan, A., & Danese, L. 2004, ApJ, 600, 580

Kaneda, H., Honaka, T., Sakon, L., et al. 2008, ApJ, 684, 270

Khochfar, S., Emsellem, E., Serra, P., et al. 2011, MNRAS, 417, 845

Kormendy, J., Fisher, D. B., Cornell, M. E., & Bender, R. 2009, ApJS, 182, 216

Krajnović, D., Bacon, R., Cappellari, M., et al. 2008, MNRAS, 390, 93

Krajnović, D., Alatalo, K., Blitz, L., et al. 2013a, MNRAS, 432, 1768

Krajnović, D., Karick, A. M., Davies, R. L., et al. 2013b, MNRAS, 433, 2812

Lauer, T. R. 2012, ApJ, 759, 64

Lauer, T. R., Faber, S. M., Holtzman, J. A., et al. 1991, ApJ, 369, L41

Lauer, T. R., Faber, S. M., Currie, D. G., et al. 1992, AJ, 104, 552

Macchetto, F., Pastoriza, M., Caon, N., et al. 1996, A&A, 120, 463

Malin, D. F., & Carter, D. 1983, ApJ, 274, 534

Marino, A. Iodice, E., Tantalo, R., et al. 2009, A&A, 508, 235

Marino, A., Rampazzo, R., Bianchi, L., et al. 2011, MNRAS, 411, 311

Mihos, J. C. 2004, in Clusters of Galaxies: Probes of Cosmological Structure and Galaxy Evolution (Cambridge, New York: Cambridge University Press), 277

Nanni, A., Bressan, A. Marigo, P., & Girardi, L. 2013, MNRAS, 434, 2390

Phillips, M. M., Jenkins, C. R., Dopita, M. A., Sadler, E. M., & Binette, L. 1986, AJ, 91, 1062

Panuzzo, P., Vega, O., Bressan, A., et al. 2007, ApJ, 656, 206

Panuzzo, P., Rampazzo, R., Bressan, A., et al. 2011, A&A, 528, A10

Pellegrini, S. 2010, ApJ, 717, 640

Pinkney, J., Gebhardt, K., Bender, R., et al. 2003, ApJ, 596, 903

Rampazzo, R., Marino, A., Tantalo, R., et al. 2007, MNRAS, 381, 245

Rampazzo, R., Panuzzo, P., Vega, O., Bressan, A., & Clemens, M. 2013, MNRAS, 432, 374

Salim, S., & Rich, R. M. 2010, ApJ, 714, L290

Sandage, A., & Tammann, G. A. 1987, Carnegie Institution of Washington Publication, 2nd edn. (Washington: Carnegie Institution)

Sansom, A. E., Hibbard, J. E., & Schweizer, F. 2000, AJ, 120, 1946

Sarzi, M., Falcón-Barroso, J., Davies, R. L., et al. 2006, MNRAS, 366, 1151

Sarzi, M., Shields, J. C., Schawinski, K., et al. 2010, MNRAS, 402, 2187

Serra, P., Trager, S. C., Oosterloo, T. A., & Morganti, R. 2008, A&A, 483, 57

Serra, P., Oosterloo, T. A., Morganti, R., et al. 2012, MNRAS, 422, 1835

Serra, P., Oser, L., Krajnović, D., et al. 2014, MNRAS, 2014, submitted [arXiv:1401.3180]

Tal, T., van Dokkum, P. G., Nelan, J., & Bezanson, R. 2009, AJ, 138 1417

Thilker, D. A., Bianchi, L., Schiminovich, D., et al. 2010, ApJ, 714, L171

Thomas, D., Maraston, C., & Bender, R. 2005, ApJ, 621, 673

Treu, T., Ellis, R. S., Liao, T. X., et al. 2005, ApJ, 633, 174

Turner, M., Côté, P., Ferrarese, L., L., et al. 2012, ApJS, 203, 5

van Dokkum, P. G. 2005, AJ, 130, 2647

Vega, O., Bressan, A., Panuzzo, P., et al. 2010, ApJ, 721, 1090

Yan, R., Newman, J. A., Faber, S. M., et al. 2006, ApJ, 648, 281